A bioreactor study of the metabolic repertoire and morphology of actinomycete *Streptomyces rimosus* ATCC 10970 under various initial concentrations of carbon and nitrogen sources

Marcin BIZUKOJĆ* [ID], Anna ŚCIGACZEWSKA [ID], Tomasz BORUTA [ID],
Agnieszka RUDA, Aleksandra KAWKA

Lodz University of Technology, Faculty of Process and Environmental Engineering, Department of Bioprocess Engineering, Wólczańska 213, 93-005 Łódź, Poland

* Corresponding author, e-mail:
marcin.bizukojc@p.lodz.pl

Abstract

This work aims at investigating the influence of the initial concentrations of carbon (glucose) and organic nitrogen (yeast extract) sources on *Streptomyces rimosus* ATCC10970 secondary metabolism in stirred tank bioreactors. Additionally, glucose utilisation, biomass formation, pH, redox potential and dissolved oxygen levels, and morphological development of *S. rimosus* pseudomycelium were studied. Eighteen secondary metabolites were detected by mass spectrometry and identified with the use of the authentic standard, or putatively with the use of literature and database of secondary metabolites. Varied initial yeast extract concentration acted much stronger on the formation of secondary metabolites than glucose did. For example, oxytetracycline was not biosynthesised at high yeast extract concentration while the formation of three other metabolites was enhanced under these conditions. In the case of glucose its increasing initial concentration led to higher secondary metabolite levels with the exception of an unnamed angucycline. High initial yeast extract concentration also drastically changed *S. rimosus* pseudomycelial morphology from the pelleted to the dispersed one. Ultimately, the cultivation media with the varied initial levels of carbon and nitrogen sources were proved to have a marked effect on *S. rimosus* secondary metabolism and to be the simplest way to either induce or block the formation of the selected secondary metabolites.

Keywords

actinomycete, batch bioreactor, secondary metabolites, *Streptomyces rimosus*, microbial morphology

1. INTRODUCTION

A number of pharmaceutically relevant metabolites and enzymes are produced by various filamentous microorganisms like moulds (filamentous fungi) and actinomycetes (filamentous gram-positive bacteria). Their rich secondary metabolism supplies substances of high biological activity and often of industrial importance (Del Carratore et al., 2022; Seca and Pinto, 2019).

Streptomyces rimosus is a profound representative of actinomycetes. It is mostly recognized for its ability to produce a widely used antibacterial antibiotic oxytetracycline, which is also known under the name of terramycin (Petković et al., 2017; Stephens, 1952). Previous studies revealed that oxytetracycline is not the sole product biosynthesized by this microorganism under the conditions of stirred tank bioreactor cultivation. *Streptomyces rimosus* is capable of producing more than ten secondary metabolites, which can be putatively identified with the use of mass spectrometry techniques and databases of secondary metabolites upon the monoisotopic masses of ions m/z (Boruta et al., 2021). The rich

metabolism of *S. rimosus* ATCC10970 was also confirmed by genome sequencing (Pethick et al., 2013). The large number of *S. rimosus* secondary metabolites is associated with its life conditions in the soil, where they serve as efficient chemical weapons against other living organisms. *Streptomyces rimosus* efficiency to compete against other microbes is very high as it was previously observed in the co-cultivations of *S. rimosus* with filamentous fungi and other actinomycete (Boruta and Ścigaczewska, 2021; Boruta et al., 2021).

With regard to *S. rimosus* and oxytetracycline production there are few older papers that focused on the bioprocess issues of oxytetracycline production, including the effect of medium composition on its formation. In one of the earliest works Zygmunt (1961) studied the influence of protein amino acids, carbohydrates and organic acids on the production of oxytetracycline in the scale of shake flasks. Abou-Zeid et al. (1977) worked on the production of oxytetracycline with the use of industrial by-products as substrates. Later Abou-Zeid et al. (1981) focused on the effect of various nitrogen sources on oxytetracycline production. Ogaki et al. (1986) studied the production of oxytetracycline by growing immobilised

S. rimosus cells in the continuous bioreactor. Later, scientists mainly focused on the genetic issues ruling the biosynthesis of this valuable metabolite. The work by Yu et al., (2012) concerned the duplication of minimal polyketide synthase genes involved in oxytetracycline production by *S. rimosus*. Yin et al. (2017) studied the increase of the resistance of *S. rimosus* towards oxytetracycline by genetic manipulations. Only Singh et al. (2012) optimised the medium with the key components, i.e. glucose, calcium carbonate and soybean oil for a new *S. rimosus* isolate with the use of the response surface methodology. Ramasamy et al. (2014) also statistically optimised the medium for oxytetracycline production using a novel cellulose-rich plant substrate from *Prosopsis juliflora*.

Several articles concerned the production of rimocidin, which is an antifungal polyketide from *S. rimosus* (Jiang et al., 2022; Li et al., 2023; Zhao et al., 2019). Nevertheless, these authors mainly focused on the genetic mechanisms ruling its biosynthesis (Jiang et al., 2022; Zhao et al. 2019) and none of these studies were made in the scale of bioreactors. Furthermore, they only studied rimocidin, while Seco et al. (2004) and Boruta et al. (2021) found that there were three rimocidins produced by *S. rimosus* with various length of the side chain at the 27th carbon atom.

Regarding other metabolites from *S. rimosus* Li et al. (2022) revealed the cryptic genes in *S. rimosus* responsible for momomycin biosynthesis, but this work did not deal with the production of this metabolite in the bioreactor either. McClure et al. (2016) found rimosamide A and B gene clusters in various *S. rimosus* strains but their study did not deal with seeking the conditions to biosynthesise these non-ribosomal peptides.

There are several studies associating the morphology of the actinomycete pseudomycelium and the formation of secondary metabolites. For example, Jonsbu et al., (2002) claimed that pelleted morphology did not support the formation of nystatin by *S. noursei*, while for the formation of niccomycin by *S. tendae* the pelleted morphology was optimal (Vecht-Lifshitz et al., 1992). The production of rebeccamycin by *Lentzea aerocolonigenes* (Dinius et al., 2023) and labyrinthopeptin A1 by *Actinomadura namibiensis* (Tesche et al., 2019) also strongly depended on the pseudomycelial morphology but in both these works it was controlled by morphological engineering techniques involving either microparticle or salt addition. As seen upon the examples above, all these works dealt with the individual secondary metabolites and species other than *S. rimosus* actinomycete were the objects of the studies.

As the most fundamental approach to stimulate microorganisms for the production of secondary metabolites is the manipulation of growth conditions and media composition (Bode et al. 2002) and the amounts of carbon and nitrogen sources are one of the strongest factors influencing secondary metabolism, it is clear that these types of experiments might reveal yet unveiled data on the studied microorganisms. It was found in the literature that there has been a limited number of studies on the effect of carbon and nitrogen concentration on the production of the individual secondary metabolites, like oxytetracycline or rimocidin, by *S. rimosus* so far. What is more, no works that joined this fundamental effect with more than one secondary metabolite at a time can be found, leaving alone their association with the microbial morphology. That is why this work is aimed at studying the influence of the initial yeast extract and glucose concentration on the formation of eighteen metabolites (confirmed and putative) of *S. rimosus* and morphological development of this actinomycete in the stirred tank bioreactor cultivations.

2. MATERIALS AND METHODS

2.1. Microorganism

Streptomyces rimosus ATCC 10970 strain was purchased from the American Type Culture Collection (ATCC) and was stored on agar slants according to the ATCC instructions. Before each experiment fresh 10-day slants were developed. The arthrospores from the slants were washed into the bottles with 300 mL cultivation medium. This suspension served as the inoculum and was directly pumped into three individual bioreactors for each series of experiments. Spore concentration in the bioreactor was each time equal to 10^9 L^{-1} and was controlled by their enumeration in a Thoma chamber.

2.2. Medium composition and process conditions

The initial composition of the cultivation media differed in each bioreactor with regard to carbon (glucose, GLU) and nitrogen (yeast extract, YE) source concentrations. In order to find the influence of the nitrogen and carbon sources, 20 g GLU·L^{-1} with 1, 5 and 20 g YE·L^{-1} as well as 5 g YE·L^{-1} with 0, 3.5, 7 and 20 g GLU·L^{-1}, respectively, were applied (Table 1).

The other ingredients of the medium were as follows: KH_2PO_4 1.51 g·L^{-1}, NaCl 0.4 g·L^{-1}, $MgSO_4 \cdot 7H_2O$ 0.5 g·L^{-1}, $ZnSO_4 \cdot 7H_2O$ 1 g·L^{-1}, $Fe(NO_3)_3 \cdot 9H_2O$ 2 g·L^{-1}, biotin 0.04 mg·L^{-1}. The solution of trace elements was added at a concentration 1 ml·L^{-1} and contained $MnSO_4$ 50 mg·L^{-1}, $Na_2B_4O_7 \cdot 10H_2O$ 100 mg·L^{-1}, $CuSO_4 \cdot 5H_2O$ 250 mg·L^{-1} and $Na_2MoO_4 \cdot H_2O$ 50 mg·L^{-1}. The initial pH level was set to 6.3 with the use of sodium hydroxide solution. The media were sterilized at 121 °C.

Six bioreactor experiments were carried out with varied initial yeast extract and glucose concentrations. Three stirred tank BIOSTAT®B bioreactors (Sartorius, Germany) were simultaneously used. They were equipped with standard dissolved oxygen, pH and redox potential sensors. The working volume of each bioreactor was 5.5 L. Dissolved oxygen level was not controlled so that the influence of mechanical stress towards growing cells was identical in each bioreactor. It was required to study the morphological development of *S. rimosus* pseudomycelium. The following aeration sequence, identical in each

Table 1. Medium composition in the performed experiments.

Initial glucose concentration (g GLU·L^{-1})	Initial yeast extract concentration (g YE·L^{-1})	Data used for the study of...
20	1	...influence of nitrogen source
20	5	...influence of nitrogen/carbon source
20	20	...influence of nitrogen source
0	5	...influence of carbon source
3.5	5	...influence of carbon source
7	5	...influence of carbon source

bioreactor was set. Air flow rate was equal to 2.5 L$_{air}$ min^{-1} within the first 24 hours of the experiment and increased to 5.0 L$_{air}$ min^{-1} later on. It remained on this level until the end of the experiment. Stirring speed was constant at 220 min^{-1} within the whole duration of the experiment (Fig. 1).
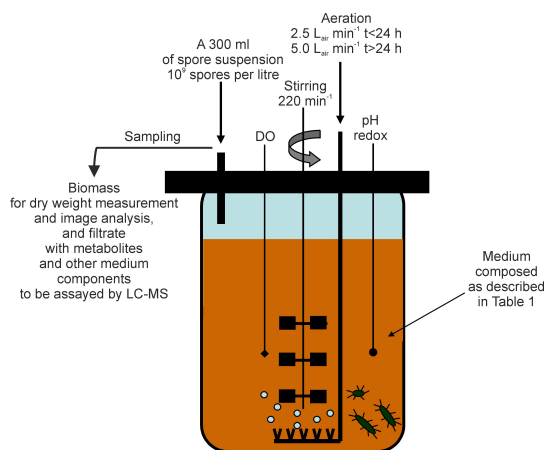

Figure 1. Bioreactor scheme.

2.3. Determination of substrates, biomass and secondary metabolites

Samples of the cultivation broth were taken every 24 hours of the experiment. In order to determine biomass content (X) on a dry mass basis they were filtered with the use of preweighed and dried at 110 °C Munktell filter discs (grade 389.84 g m^{-2}, diameter 150 mm). Filter discs with biomass were then weighed on the laboratory balance after filtration. Analysis was made in triplicates. Visual, namely naked eye and microscopic (in case of doubts), control was made to assure the filtrates were clear and contained no biomass. It confirmed the accuracy of dry weight measurements. The filtrates were then stored at −20 °C until consecutive chromatographic analyses.

The secondary metabolites present in the filtrates were analysed by ultrahigh performance liquid chromatography (AQUITY-UPLC®) with the use of BEH Shield RP18 reversed phase column (2.1 mm × 100 mm × 1.7 μm), paired with high-resolution mass spectrometry (ACQUITY-SYNAPT G2, Waters, USA). Eluent flow rate was 0.2 ml·min^{-1} and column

temperature was kept at 40 °C. The acetonitrile:water gradient (both acidified with formic acid 0.1% v/v) was set as follows: 0.0 min 0:100 (v/v), 2.0 min 0:100 (v/v), 2.5 min 20:80 (v/v), 5.5 min 30:70 (v/v), 7.5 min 40:60 (v/v), 13.8 min 60:40 (v/v), 14.0 min 60:40 (v/v). Before injection the samples were pre-treated with 0.2 μm syringe filters. Monoisotopic masses of the ions were measured with the use of mass spectrometry in the negative and positive ionisation mode. The detailed setup of mass spectrometer was described elsewhere (Boruta et al., 2021). Metabolites were studied semi-quantitatively by considering their peak areas of [M−H]$^-$ or [M+H]$^+$ ions. This analysis was conducted with the use of TargetLynx (Waters, USA) software. The sensitivity of semi-quantitative analysis was 10 auxiliary units (AU). This level allowed us to confirm the presence of a given secondary metabolite in the cultivation broth. For oxytetracycline quantitative analysis was performed with the use of the authentic standard. The identification of other ions was based on their monoisotopic mass values (m/z). Metabolites were sought with the use of Natural Product Atlas (van Santen et al., 2022) considering their origin from *Streptomyces* genus. Absolute error $\Delta(m/z)$ was determined by subtracting the theoretical m/z from the experimental m/z and it had to be lower than $|\pm 0.009|$ to accept the putative identification of the given ion.

Glucose concentration in the filtrates was determined with the use of ultrahigh performance liquid chromatography (AQUITY-UPLC®) by applying BEH Amide normal phase column (2.1 mm × 150 mm × 1.7 μm), paired with Evaporative Light Scattering Detector (Waters, USA). Glucose was eluted with 75% acetonitrile dissolved in deionised water enriched with 0.2% triethylamine. The parameters of the analysis were as follows: eluent flow rate 0.29 ml·min^{-1} and column temperature 35 °C. All chromatographic analyses were made in triplicates.

The morphological analysis of *S. rimosus* pseudomycelial objects was made in the samples collected from the bioreactor every 24 hours. The vital slides were prepared and observed with the use of light phase contrast microscope (OLYMPUS BX53, Olympus Corporation, Japan) and the high-resolution RGB digital camera (OLYMPUS DP27). All taken images were processed and analyzed with the use of image analysis software (OLYMPUS cellSens Dimension Desktop 1.16, Olympus Corporation, Japan). The semiautomatic image processing and

analysis procedure included the application of the median filter and Sobel filter to, respectively, remove noise from the images and detect the edges of the pseudomycelial objects. In the second part of the procedure two fractions of *S. rimosus* objects were distinguished based on their shape and size: (1) the fully evolved pellets and (2) the hyphae and clumps. This semiautomatic image processing and analysis procedure were described in detail elsewhere (Kowalska et al., 2018; Ścigaczewska et al., 2021). As a result, the values of three morphological parameters, namely the projected area (A), elongation (E) and morphology number (Mo), defined by Wucherpfennig et al. (2011), were obtained. Their detailed description was provided by Kowalska et al. (2018). Mean values of morphological parameters were calculated on the basis of at least 30 actinomycete objects to assure the statistically significant data.

3. RESULTS

As it is common knowledge that the initial amounts of available nitrogen and carbon source are the primary factors to influence the run of any process with the participation of heterotrophic microorganisms, it was expected that the final outcome of *S. rimosus* bioreactor cultivations would be strongly affected by them.

3.1. Substrate uptake and biomass formation

Low initial amount of yeast extract at the level of $1 \, \text{g YE·L}^{-1}$ led to strongly nitrogen-limited growth of biomass whose amount did not exceed $2 \, \text{g X·L}^{-1}$ within the duration of the process (96 hours) and as a consequence hardly any glucose was utilised therein. At higher initial yeast extract concentrations (5 and $20 \, \text{g YE·L}^{-1}$) utilisation of glucose was not affected, while high amount of nitrogen source ($20 \, \text{g YE·L}^{-1}$) at the beginning of the processes resulted in more than doubling (compared to $5 \, \text{g YE·L}^{-1}$ of biomass amount at 96 hour of the run (Fig. 1).

The effect of varied initial glucose concentration (carbon source) was not as spectacular as that of nitrogen source. In the process without glucose less than $2 \, \text{g·L}^{-1}$ of biomass was formed. When the initial glucose concentration increased, the amount of biomass formed was proportionally higher, although at $20 \, \text{g GLU·L}^{-1}$ its content was not as high as one might have expected, if direct proportionality was taken into account. The shapes of curves to show glucose temporal changes were similar for the processes with the initial glucose concentrations from 3.5 to $20 \, \text{g GLU·L}^{-1}$ because they were practically parallel to each other (Fig. 2).
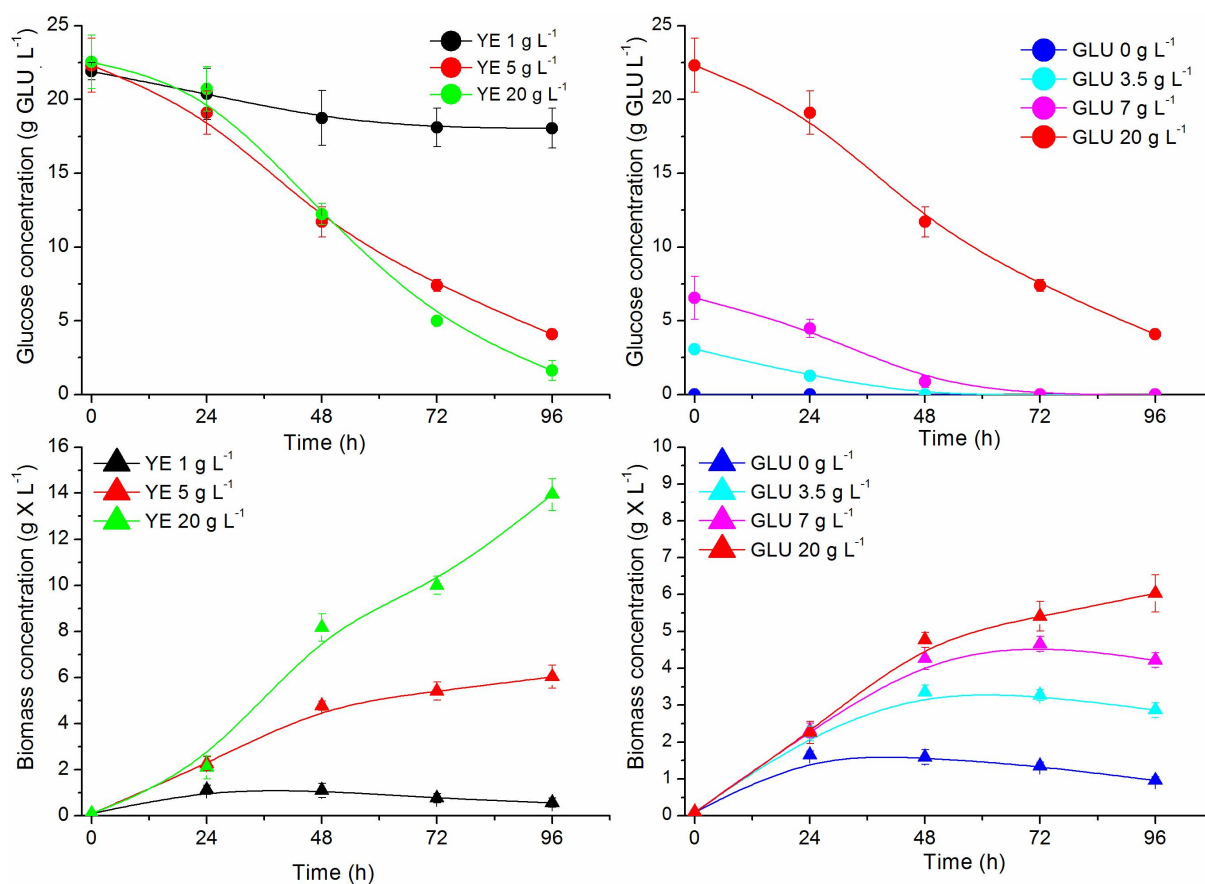

Figure 2. Influence of initial glucose and yeast extract concentration on the temporal changes of glucose and biomass concentrations; error bars indicate standard deviation of the triplicated analysis.

3.2. Temporal changes of dissolved oxygen, pH and redox potential

With regard to dissolved oxygen (DO) profiles the analysis was made only in the first 36 hours of the processes because in the later hours of the experiments the DO probe readouts were biased by biomass covering the tip of oxygen sensor (Fig. 3).

The change of the initial glucose concentration did not markedly influence DO profiles. Only in the run without glucose DO abruptly increased after 24 hours due to the deficiency of yeast extract that must have played the role of carbon source while glucose was absent. At the lowest yeast extract concentration DO decreased slower in the first 12 hours of the run compared to the processes with 5 and 20 g YE·L^{-1} (Fig. 3).

On the other hand, the effect of varied initial carbon and nitrogen source concentration on pH profiles was amazingly strong. In all cases the decrease of pH level was generally observed around 24 hour of all runs. But at 20 g YE·L^{-1} it went down to the value of 4.8 while in the two other runs it remained between 6.4 and 6.7 in the last hour of the process. When no glucose was added to the medium, pH level did not decrease around 24 hour of the run and it was the only case out of all runs. Next its level was simultaneously increasing up to the pH level above 8.1, which was the highest value out of all experiments made. Generally, the lower initial glucose concentration, the lower the level of pH at 96 hour of the process.

The varied initial glucose concentration had hardly any effect on the redox potential level. Its profiles were similar with the characteristic region of negative values around 24 hour of the process, the period of time in which actinomycete growth was the most intensive. The effect of the initial yeast extract concentration was similar with regard to the shape of the curve, but when it was equal to 20 g YE·L^{-1}, the values of redox potential remained negative until the end of the process. Furthermore, at 1 g YE·L^{-1} no negative values of redox potential were noted. All in all, the changes of redox potential values clearly reflected the activity of *S. rimosus* under studied conditions. Its lowest negative values showed the moment (at about 24 hour) of the most intensive pseudomycelial growth and oxygen utilisation. It was correlated with DO values at this hour. In that moment of the experiment the conditions seemed to be tending to the microaerobic ones for a short period of time. The values of redox potential also showed that the high activity of *S. rimosus* in the nitrogen-richest medium lasted until the end of experiment (its aforementioned negative values noted until 96 hour). It could not be tracked with DO probe due to its biased readouts caused by the intensive pseudomycelial growth. Last but not least, the low activity of *S. rimosus* at nitrogen limiting conditions (1 g YE·L^{-1}) was also indicated by the lack of the negative values of redox potential.

3.3. Secondary metabolites

In all bioreactor experiments with *S. rimosus* eighteen secondary metabolites were detected in the cultivation broths. In Table 2 they are all listed and shortly described with the special attention to the *Streptomyces* species in which they were previously reported.

Streptomyces rimosus was able to biosynthesise many substances of various biochemical origin and biological activities (Table 2). These were antibiotic macrolides like rimocidins, milbemycin a$_3$ and oxidised milbemycins, lucensomycin, non-ribosomal peptides like rimosamides and siderophoric turigichelin, an oxazine antibiotic spinoxazine, aminoglucoside antibiotics 7-demethyl-glucopiericidin A, an anthraquinone derivative like an unnamed angucycline, an adenine derivative like 2-methylthio-cis-zeatin, aromatic acids like lorneic acid J and enaminomycin B, and, last but not least, naphthacene antibiotics like oxytetracycline and 2-acetyl-2-decarboxamido-oxytetracycline.

High initial nitrogen concentration did not favour the production of secondary metabolites from the oxytetracycline group. Neither oxytetracycline nor 2-acetyl-2-decarboxamidooxytetracycline were detected at 20 g YE·L^{-1}. Low organic nitrogen level of 1 g YE·L^{-1} favoured more 2-acetyl-2-decarboxamidooxytetracycline than oxytetracycline. There was a clear correlation for three detected rimocidins. For all of them the initial nitrogen concentration of 5 g YE·L^{-1} was the optimal value. So it was for turigichelin, lucensomycin, an unnamed angucycline and 7-demethylglucopiericidin A (Fig. 4).

It was almost like above for milbemycin a$_3$ and oxidised milbemycins, although for milbemycin a$_3$+4[O] its levels were comparable for both 1 and 20 g YE·L^{-1}. Both rimosamides A and B showed similar characteristic temporal changes with a strong peak at about 48 hour at 5 g YE·L^{-1} and it also seemed to be the optimum nitrogen concentration for these metabolites. Four other metabolites indicated a completely different correlation with the changes of the initial organic nitrogen concentration. These were lorneic acid J, enaminomycin B, spinoxazine A and 2-methylthio-cis-zeatin. Their levels at 1 g YE·L^{-1} were close to zero and their highest signals were detected for the highest initial nitrogen concentration of 20 g YE·L^{-1} (Fig. 4)

The effect of the initial glucose concentration on the levels of secondary metabolites was more predictable (Fig. 5). Their production is known to be strongly carbon source dependent as these are the carbon atoms that make a complicated carbon skeleton of these relatively large molecules. So in the case of 17 out of 18 detected metabolites their signals were the highest at 20 g GLU·L^{-1}. The only exception was an unnamed angucycline whose quadrupled level compared with the other runs was astonishingly obtained when no glucose was present in the medium.
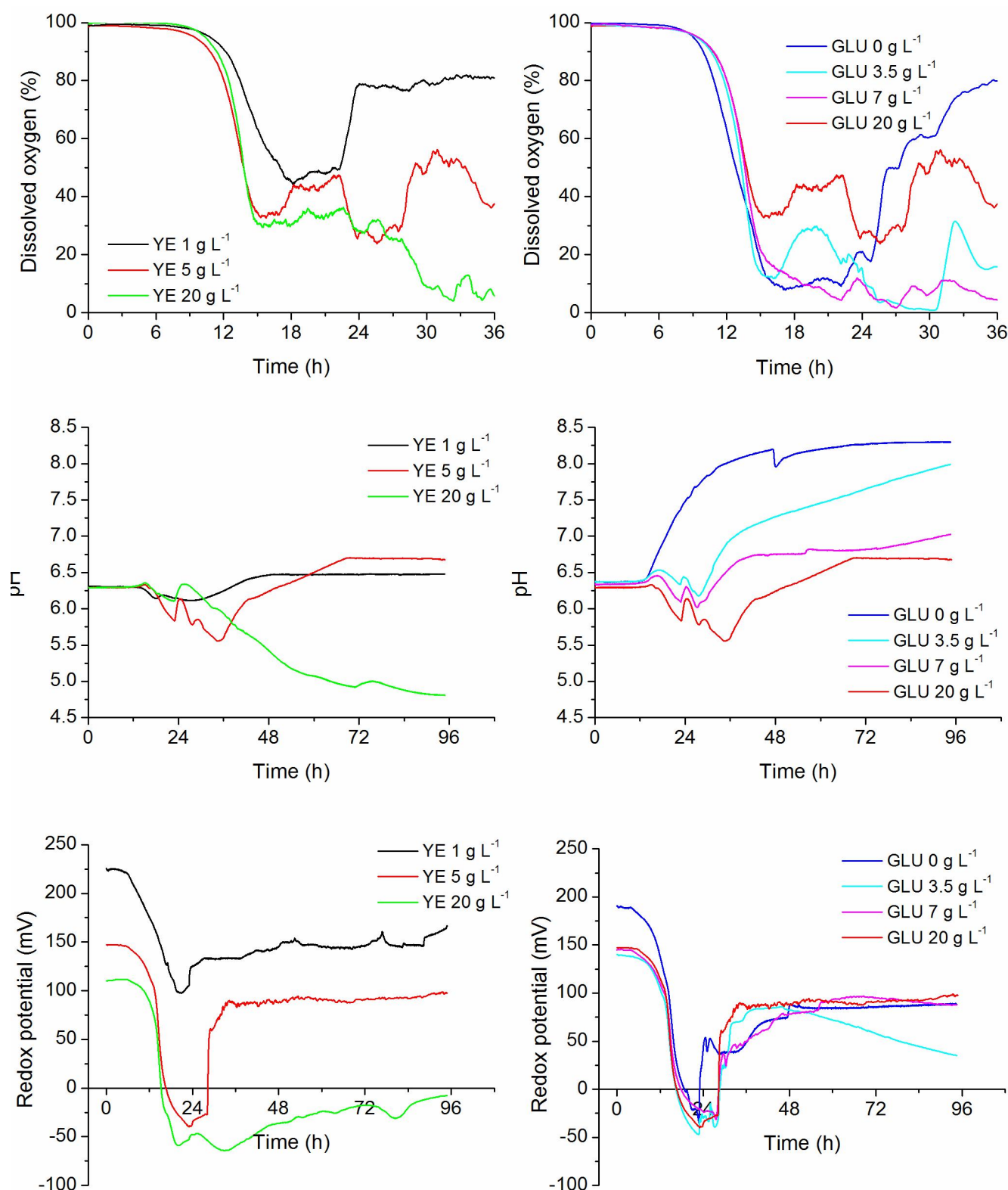
Figure 3. Influence of initial glucose and yeast extract concentration on temporal changes of dissolved oxygen, pH and redox potential.

In several cases the lack of glucose inhibited the production of metabolites and these were 2-acetyl-2-decarboxamido-oxytetracycline, łorneic acid J, enaminomycin B and spinoxazine A. The least clear correlation was found for both rimosamides. Although their highest levels were detected for 20 g GLU·L^{-1}, the second in the row were the runs without glucose, in which the levels of these metabolites were only slightly lower than those at 20 g GLU·L^{-1}, especially in the case of rimosamide A (Fig. 5).

Table 2. List of secondary metabolites of *S. rimosus* detected in the cultivation broths.

No.	$(m/z)_{exp.}$	Assigned formula [M−H]$^-$	$(m/z)_{theor.}$	Absolute error $\Delta(m/z)$	Assigned secondary metabolite	Type and origin of metabolite	Literature
1	459.1427	$C_{22}H_{23}N_2O_9$	459.1404	+0.0023	Oxytetracycline	Antibacterial from *S. rimosus*	Stephens et al. (1952)
2	458.1409	$C_{23}H_{24}NO_9$	458.1451	−0.0042	2-Acetyl-2-decarboxamido-oxytetracycline	By-product from *S. rimosus*	Hochstein et al. (1960)
3	619.3103	$C_{24}H_{43}N_8O_{11}$	619.3051	−0.0052	Turgichelin	Siderophore from *S. antibioticus* NBRC 13838	Kodani et al. (2013)
4	766.3990	$C_{39}H_{60}NO_{14}$	766.4014	−0.0024	Rimocidin	Antifungal from *S. rimosus*	Seco et al. (2004)
5	738.3635	$C_{37}H_{56}NO_{14}$	738.3701	−0.0066	Rimocidin CE-108	Antifungal from *S. rimosus*	Seco et al. (2004)
6	752.3879	$C_{38}H_{58}NO_{14}$	752.3857	+0.0022	Rimocidin (27-ethyl)	Antifungal from *S. rimosus*	Boruta et al., (2021)
7	527.2993	$C_{31}H_{43}O_7$	527.3009	−0.0016	Milbemycin a$_3$	Antifungal from *S. hygroscopicus*	Nonaka et al. (2000)
8	591.2823	$C_{31}H_{43}O_{11}$	591.2805	+0.0018	Milbemycin a$_3$ + [4O]	Antifungal from *S. hygroscopicus*	Nonaka et al. (2000)
9	593.3038	$C_{31}H_{45}O_{11}$	593.2962	+0.0076	Milbemycin β$_{11}$ + [4O]	Antifungal from *S. hygroscopicus*	Nonaka et al. (2000)
10	708.3666*	$C_{36}H_{54}NO_{13}$*	708.3595	+0.0071	Lucensomycin	Antibacterial from *S. lucensis*	Manwaring et al. (1969)
11	603.3022	$C_{30}H_{43}N_4O_9$	603.3030	−0.0008	Rimosamide A	A non-ribosomal peptide from *S. rimosus*	McClure et al. (2016)
12	589.2874	$C_{29}H_{41}N_4O_9$	589.2854	+0.0020	Rimosamide B	A non-ribosomal peptide from *S. rimosus*	McClure et al, (2016)
13	229.1228	$C_{15}H_{17}O_2$	229.1221	+0.0008	Lorneic acid J	Tyrosinase inhibitor from *Streptomyces* sp. KIB-H1289	Yang et al. (2017)
14	240.0508	$C_{10}H_{10}NO_6$	240.0492	+0,0016	Enaminomycin B	Antibacterial from *S. baarnensis* No. 13120	Itoh et al. (1978)
15	263.1064	$C_{13}H_{15}N_2O_4$	263.1032	+0.0032	Spinoxazine A	Widely active antibiotic from *S. spinoverrucosus* SNB-048	Fu et al. (2016)
16	264.0859	$C_{11}H_{14}N_5OS$	264.0919	−0.0060	2-Methylthio-cis-zeatin	A cytokinin active compound from *Rhodococcus fascians***	Armstrong et al. (1976) Lopez et al, (2022)
17	384.1161	$C_{20}H_{18}NO_7$	384.1083	+0.0078	An unnamed angucycline	Putative cytostatic from *Streptomyces* sp. QL37	Wu et al. (2019)
18	724.3525	$C_{36}H_{54}NO_{14}$	724.3544	-0.0019	7-demethylgluco-piericidin A	Antifungal from *Streptomyces* sp.KIB-H1083	Shang et al. (2018)

*In this case it was the positive ion and assigned formula is for [M+H]$^+$

**Rhodococcus fascians* belongs to the class *Actinomycetia*, the same as genus *Streptomyces*. Nevertheless its N7 methyl derivative was later found by Lopez et al. (2022) at *Streptomyces* sp.
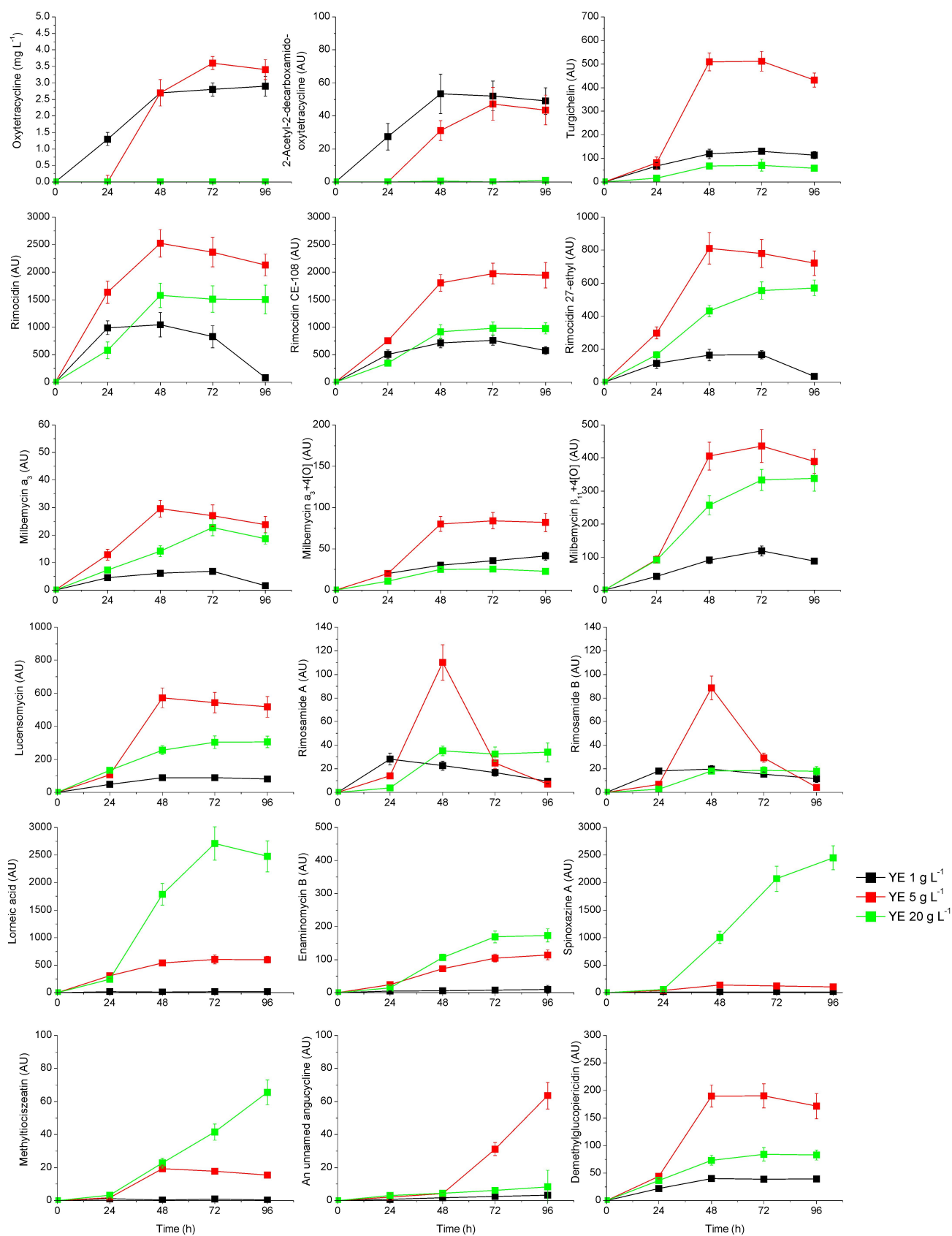
Figure 4. Influence of the initial yeast extract concentration on temporal changes of *S. rimosus* secondary metabolites; error bars indicate standard deviation of the triplicated analysis.
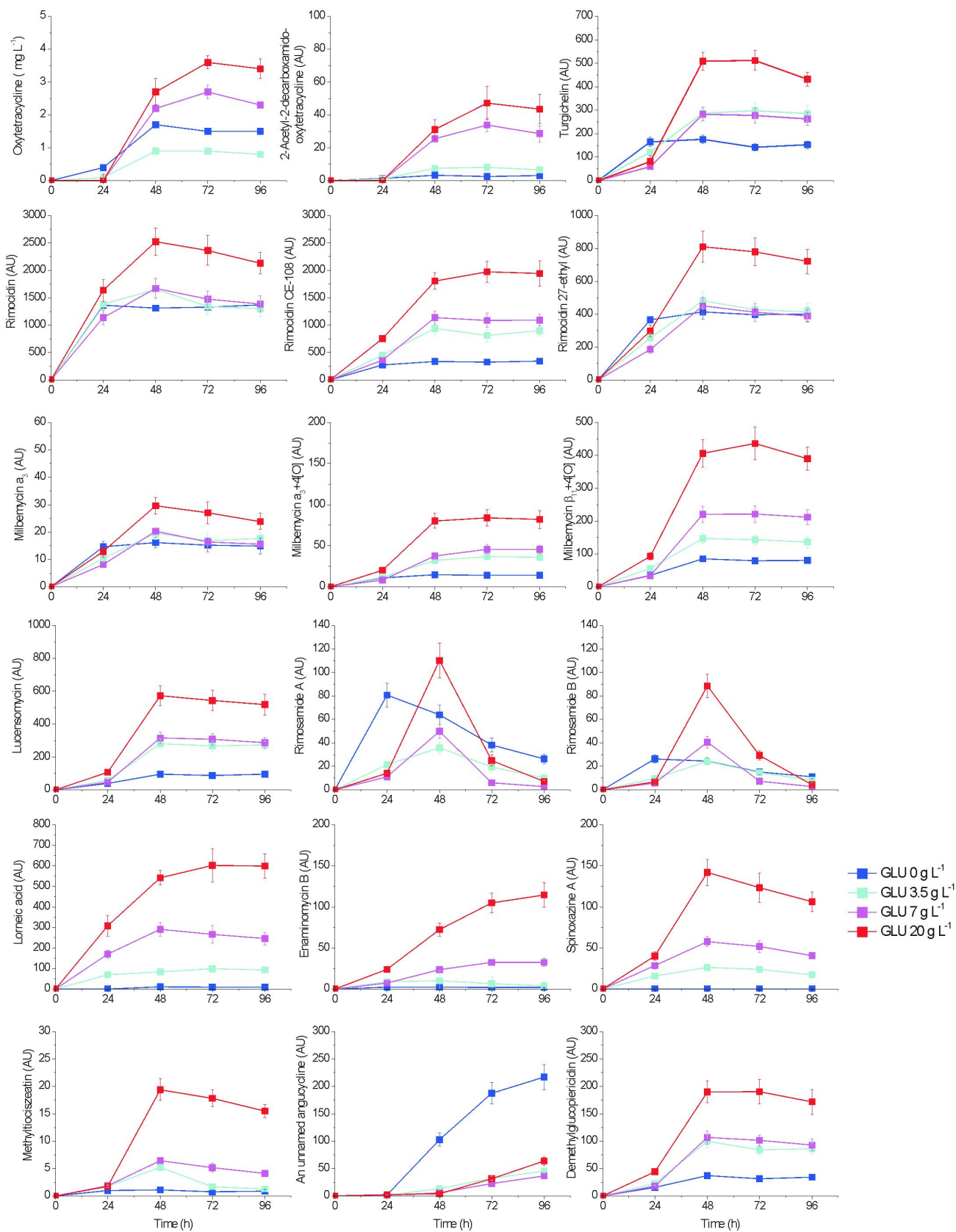
Figure 5. Influence of initial glucose concentration on temporal changes of *S. rimosus* secondary metabolites; error bars indicate standard deviation of the triplicated analysis.

3.4. *Streptomyces rimosus* pseudomycelial morphology

Being a filamentous bacterium *S. rimosus*, similarly to other filamentous organisms like fungi, forms complex structural pseudomycelial objects in submerged cultures. It can either grow in the form of pellets or show dispersed filamentous morphology. It depends on process conditions, medium composition or concentration of the inoculum. In this study it occurred that the initial concentration of both carbon and nitrogen source influenced pseudomycelial morphology of *S. rimosus*.

In all cases the following pattern of *S. rimosus* growth was observed. Within the first 24 hours after the inoculation with spore suspension it evolved towards pellets of the given size (expressed in this work by their projected area). Then the size of pellets remained generally unchanged. Furthermore, in some cases both pellets and clumps and filaments were simultaneously present.

The initial concentration of nitrogen source strongly influenced the size of the pellets. The rule was found that the lower the initial yeast extract concentration, the larger pellets evolved. Almost two magnitudes of difference in their size were measured: about $1.25 \cdot 10^5$ μm^2 at 1 g YE·L^{-1} and $3.55 \cdot 10^3$ μm^2 at 20 g YE·L^{-1}. At the lowest initial yeast extract concentration the culture contained only pellets (Fig. 6). The higher was the initial organic nitrogen concentration, the more clumps and free filaments were observed in the bioreactor (Fig. 6 and 7). For yeast extract concentration equal to 20 g YE·L^{-1} free hyphae and clumps were observed practically from 24 hour until the end of the run. What is more, pellets vanished at 20 g YE·L^{-1} already at 72 hour of the run (Fig. 7). In all cases clumps and hyphal objects were almost by three magnitudes lower (about 10^2 μm^2) than the accompanying pellets.

The effect of varied initial glucose concentration on pellet size was not as spectacular as that of the initial yeast extract concentration (Fig. 6, 7 and 8). Only the run without glucose fell apart from the other runs and pellet projected area was the highest therein. It was from 3 to $4 \cdot 10^4$ μm^2 between 24 and 96 hour of the experiment. For the initial glucose concentrations from 3.5 to 20 g GLU·L^{-1} the size of pellets was practically identical and lower (from 0.8 to $1.4 \cdot 10^5$ μm^2 starting with 48 hour of the run) than that for glucose-free variant. In all these experiments with varied initial glucose concentration clumps and filaments were observed. However, never did the pellets vanish from the cultivation broth. In all cases one observed the mixture of pellets, clumps and filaments with one exception for 20 g GLU·L^{-1} when the filaments were found only at the beginning of the process at 24 hour (Figs. 6 and 8).

The shape of pellets and filamentous objects was expressed by elongation and morphology number. Upon these parameters one can deduce to what an extent the object differed from the ideal circle or had the oval (elongated) shape.

It occurred that nitrogen deficiency favoured almost ideal circular shape of pellets in the experiment with 1 g YE·L^{-1}. Elongation was below 1.2 (1.0 is for the ideally regular object) and morphology number above 0.5 (1.0 is for the ideal sphere). Comparing this run with those started with higher initial organic nitrogen levels, there were marked differences. For the latter ones the value of elongation from 1.6 to 2.1 indicated the oval shape of pellets (at 5 and 20 g YE·L^{-1}). The value of morphology number between 0.3 and 0.4 clearly indicated that these pellets were not circular and rather of an irregular shape (Fig. 6).

With regard to the influence of the initial glucose concentration, the pellets grown on glucose-free medium differed from the other ones. They were more circular (elongation between 1 and 1.5) than those from other glucose experiments (Figs. 6 and 8). Nevertheless, the values of morphology number being sometimes close to 0.4 were relatively low. Both measured shape factors for the runs with the initial glucose concentration from 3.5 to 20 g GLU·L^{-1} were similar and no clear dependence could be found here. The shape of clumps and filaments in all runs, if they occurred, was less regular, as evidenced by higher elongation values than for pellets (Fig. 6).

The size and shape of *S. rimosus* pseudomycelial objects were also correlated with biomass concentration (Figs. 3, 6, 7 and 8). It was for the low biomass concentration (to be more precise, lower than 2 g X·L^{-1}) at nitrogen limited conditions that the pellets were larger and more regular than those observed in the other runs. They had simply more space to grow unaffected by their mutual interactions. In the case of high levels of nitrogen, a high amount of biomass grew (about 14 g X·L^{-1}) and due to the spatial limitations much smaller and less circular pseudomycelial objects, actually dispersed hyphae, were observed.

The correlation of biomass concentration with the size and shape of the mycelial objects evolved under varied initial glucose concentration was not so strong as it was in the case of varied initial yeast extract concentration. Only for glucose-free medium at low biomass concentration equal to no more than 2 g·L^{-1} the situation turned out to be similar to the nitrogen-limiting conditions. Again, circular and large pellets were formed under glucose starvation when a lot of space was left in the bioreactor. For the other initial glucose concentrations (from 3.5 to 20 g GLU·L^{-1}) biomass content was higher than that in glucose-free medium but did not differ more than about 1 g·L^{-1} between each of these runs (Fig. 3) and the mycelial objects were then similar in those runs too. However, they were smaller and less regular compared to the ones from the run with glucose concentration equal to 0 g GLU·L^{-1}.
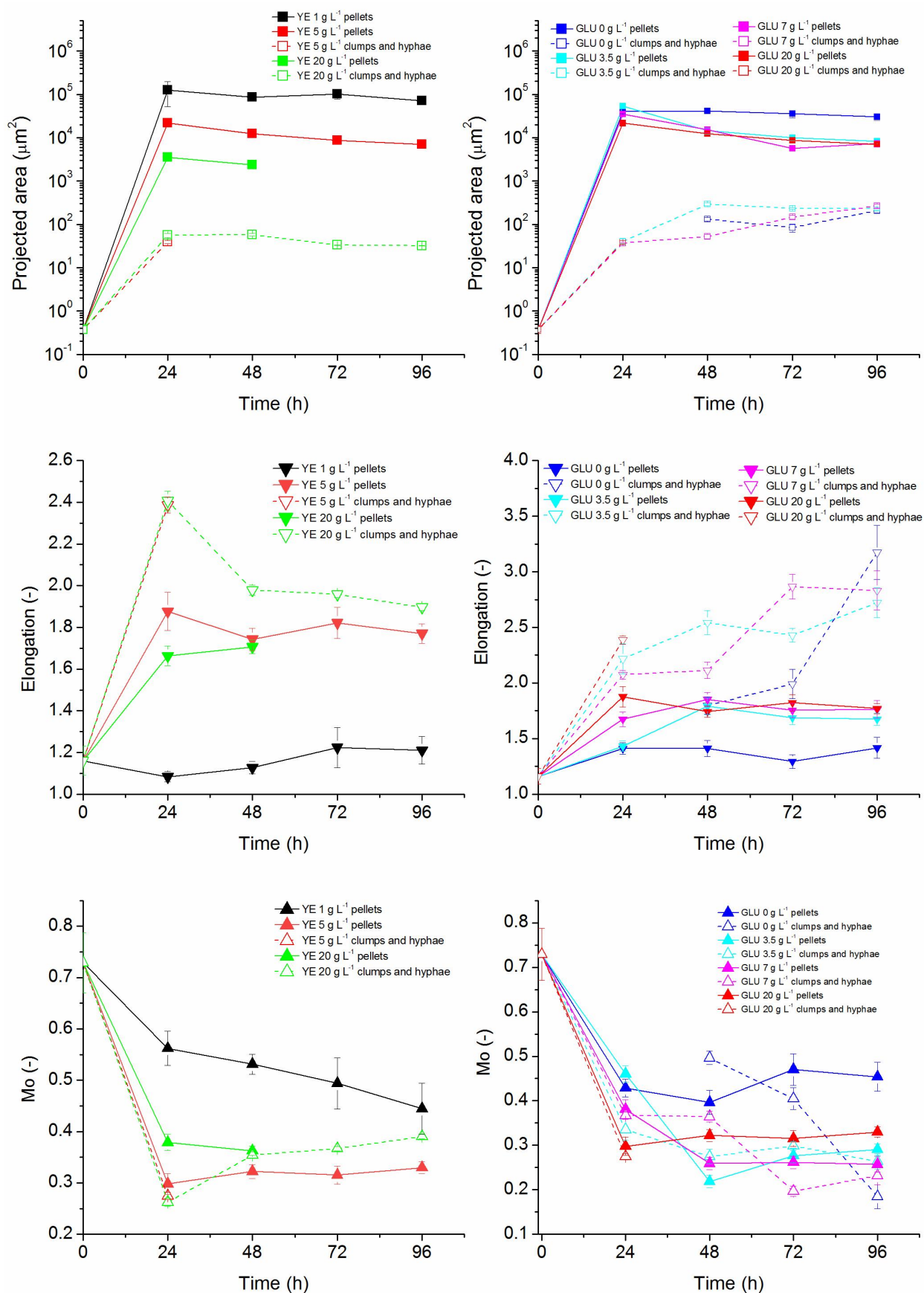
Figure 6. Influence of initial yeast extract and glucose concentrations on temporal changes of *S. rimosus* morphological parameters; error bars represent standard deviation of at least thirty pseudomycelial objects measured.
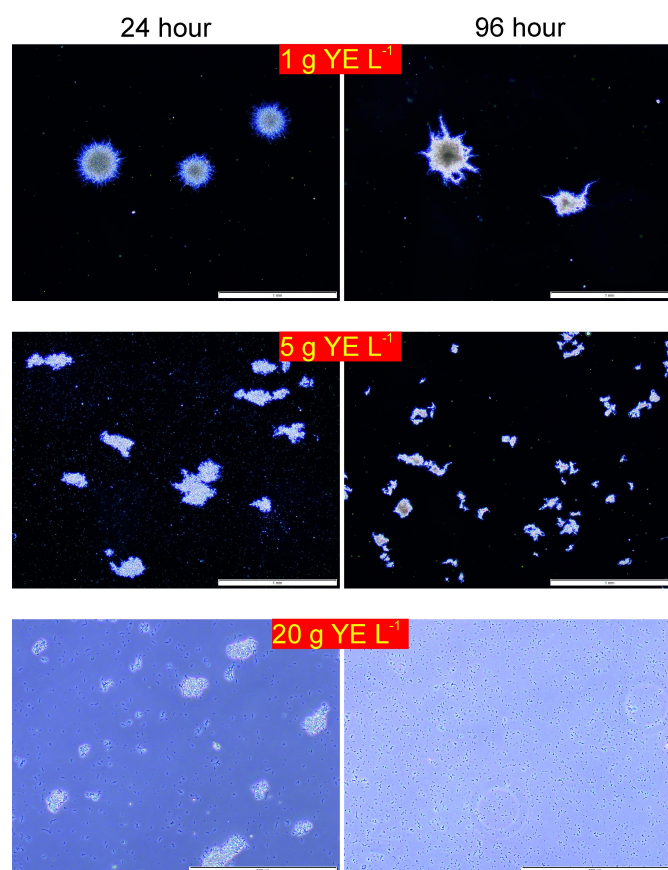
Figure 7. Images of *S. rimosus* pseudomycelial objects evolved under various initial yeast extract concentrations.

Figure 8. Images of *S. rimosus* pseudomycelial objects evolved under various initial glucose concentrations.

4. DISCUSSION

The influence of the initial carbon and nitrogen source concentration on biomass growth and glucose utilisation in the stirred tank bioreactors was typical as it is described in handbooks for bacterial cultures. When the amount of available yeast extract was low (here it was $1\,\mathrm{g\,YE{\cdot}L^{-1}}$), nitrogen source became a strongly limiting substrate ceasing both biomass growth and glucose uptake. On the other hand a low amount or lack of glucose made carbon source to be limiting and decreased the amount of biomass grown too. The changes of dissolved oxygen level and redox potential followed the curves of glucose utilisation as these three indicators are associated with microbial catabolism.

Fast increasing level of pH (even up to 8) after 24 hours in the runs without glucose and with $3.5\,\mathrm{g\,GLU{\cdot}L^{-1}}$ indicated that *S. rimosus* must have utilised yeast extract as the carbon source. It led to the deamination of amino acids to assimilate their carbon backbones and alkalisation of the medium by the release of ammonium ions. This alkalisation was worth noticing as pH level is one of the factors influencing the formation of secondary metabolites which was previously proved on the example of a polyketide mevinolinic acid (Bizukojc et al., 2012).
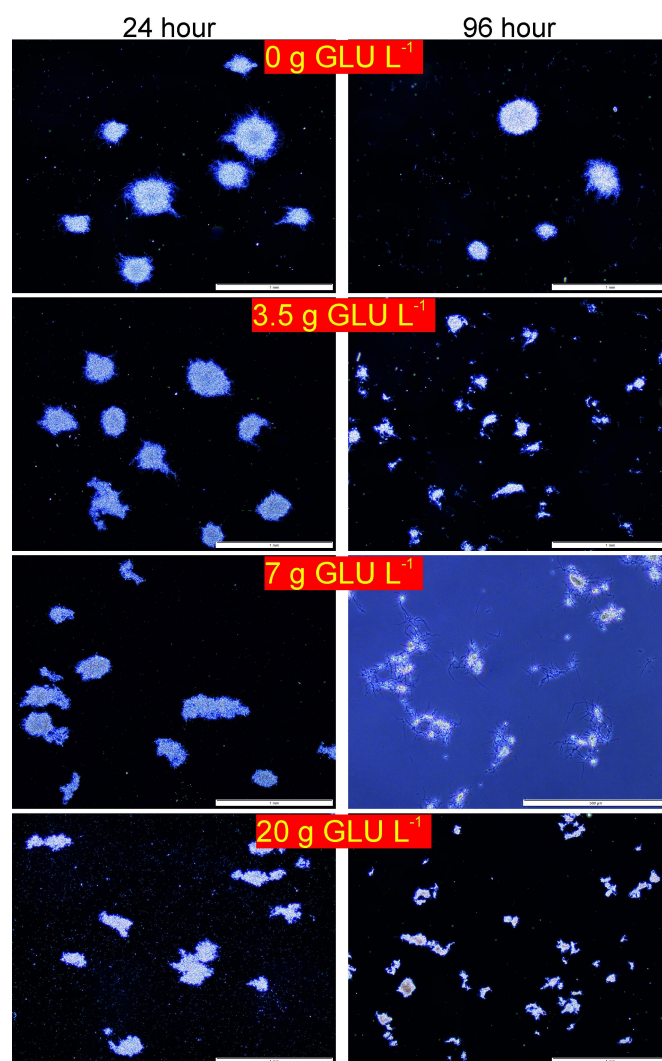
Further discussing the issue of the secondary metabolite formation, it must be once again noted that the varied initial concentration of the nitrogen source (yeast extract) far stronger affected the formation of 18 studied metabolites than the initial concentration of carbon source (glucose) did. There were four secondary metabolites, whose formation was favoured by high yeast extract concentration, namely lorneic acid J, enaminomycin A and spinoxazine A and 2-methylthio-cis-zeatin. At the same time there were metabolites which were not formed at $20\,\mathrm{g\,YE{\cdot}L^{-1}}$ at all. These were oxytetracycline and 2-acetyl-2-decarboxamidooxytetracycline. The reason could have been the drastic decrease of pH value below 5 at the highest tested initial yeast extract concentration. Although Zygmunt (1961) studied the effect of amino acid addition to the synthetic medium, he did not find any similar correlation, while Abou-Zeid et al. (1981) clearly stated that the increased amount of nitrogen source either organic or inorganic did not favour the production of oxytetracycline. It was not surprising because the effect of nitrogen source on secondary metabolism was previously described for other sec-

ondary metabolites. Fungal metabolites of *Aspergillus terreus* well exemplify this correlation as mevinolinic acid (lovastatin) is not formed at high nitrogen source concentration (yeast extract should be not higher than 4 g YE·L^{-1}) and (+)-geodin is effectively formed at highly nitrogen deficient conditions at yeast extract concentration of 2 g YE·L^{-1} (Casas López et al., 2003; Bizukojc and Ledakowicz, 2007). Nevertheless, the fact that some metabolites of *S. rimosus* namely, lorneic acid J, enaminomycin B, spinoxazine A and 2-methylthio-cis-zeatin were produced at high nitrogen concentration cannot be easily explained by the decrease of pH level. Interestingly they were not effectively formed at nitrogen deficiency either. The only common feature for these four metabolites is that they are not of polyketide origin like oxytetracycline, rimocidin, milbemycins or the aforementioned fungal metabolites. The fact that at the initial nitrogen source concentration of 20 g YE·L^{-1} pH decreased down to 5 might have been favourable for the formation of these metabolites too. But it could also be for the dispersed morphology in this run that they were effectively formed. At the same time these conditions stopped oxytetracycline formation so dispersed morphology may be unfavourable for some actinomycete antibiotics which was exemplified for nystatin production by *S. noursei* (Jonsbu et al, 2002).

The fact that increasing glucose concentration favours the formation of all secondary metabolites of tested *S. rimosus* was not surprising as any assimilated carbon source including glucose contributes to the formation of carbon backbone of these metabolites. It is a commonly known fact. For example, to produce penicillin by *Penicillium chrysogenum* high concentrations of carbon substrates (30 g·L^{-1} of sucrose and 50 g·L^{-1} of corn steep liquor and carbon substrate feeding in the fed-batch mode) are required and so is the case with the production of tetracycline (even 40 g·L^{-1} of sucrose in the mineral medium) by *S. aureofaciens* (Darken et al, 1965; Jørgensen et al., 1995). Here this rule was fully satisfied. In all cases the highest signals of all 18 secondary metabolites were found at the highest glucose level of 20 g·L^{-1}. The only exception was an unnamed compound belonging to angucyclines whose highest level was revealed in the medium without glucose at all. Angucyclines are polycyclic aromatic polyketides with four aromatic rings (benz[a]anthracene frame). However, there are insufficient literature data to interpret this result. One can only suppose that its formation might have been favoured at pH level exceeding the value of 8. In the current study this high level of pH could have been to a lower extent favourable for the formation of both rimosamides A and B too.

The effect of varied initial nitrogen and carbon source concentrations on *S. rimosus* morphology is more difficult to discuss as there are hardly any literature data concerning this species. One can refer to other organisms of genus *Streptomyces* only. For example, Jonsbu et al. (2002) analysed the production of nystatin and pseudomycelial morphology for two of *S. noursei* strains in shake flask using a variety of carbon sources (glucose, fructose and glycerol) but they did not study the effect of var-

ied carbohydrate concentration. They also observed pelleted morphology and clumps and only pellets grown on fructose were of the comparable size 10^4 μm^2 to those in the present study as the other ones were at least ten times smaller. What is more, big pellets negatively influenced nystatin formation. Yin et al. (2008) used a bioreactor for *S. avermitilis* producing avermectin but their study more concerned the effect of aeration on morphology and avermectin production which was favoured by pelleted morphology and high oxygen levels. In the case of *S. akiyoshiensis* it was phosphorus that much affected mycelial morphology and surprisingly no effect of nitrogen source on morphology was found (Yin et al., 2008).

Further discussing the issue of *S. rimosus* morphology, it must be clearly stated that in the present study mechanical stress was not the factor changing actinomycete morphology. The aeration and stirring conditions were mild and exactly the same in each bioreactor. *Streptomyces rimosus* pellet formation follows the non-agglomerative mechanisms, namely one pellet is formed from one or, more often, low number of spores (Metz and Kossen, 1977). The small size of pellets observed in this study proves it and this phenomenon is typical for *Streptomyces*. It was previously reported by Ścigaczewska et al. (2021). Furthermore, there is another factor influencing the size of *Streptomyces* pellets. It is the method of bioreactor culture initiation either from spores or from the preculture. In the case of the initiation from spores, which was the method used in the present work, the evolved pellets are always smaller than those evolved from the preculture (Ścigaczewska et al., 2021).

The deficiency of nitrogen led to the formation of larger and more circular pellets, the values of morphology number and elongation prove it, compared to those from the run with 5 g YE·L^{-1}, while the increase of the initial concentration of nitrogen to 20 g YE·L^{-1} led to their destruction and formation of dispersed morphology. As mentioned in *Results* section, low biomass content and consequently more space in the bioreactor to evolve allowed for the formation of the biggest pellets in the nitrogen deficiency experiment. Such a correlation between the amount of biomass in the association with inoculum size and pellet diameters is known for filamentous fungi (Bizukojc and Ledakowicz, 2010). The fact that it was the highest yeast extract concentration that prevented the formation of pellets remains unexplained. Here one can suppose that it could have been the result of low pH level (below 5). Low pH level leads to the formation of dispersed morphology at filamentous organisms (Papagianni, 2004).

In the conducted *S. rimosus* bioreactor cultivations it was also observed that the lack of carbon source (glucose) led to the formation of well-structured circular pellets (Figs. 6, 7). The aforementioned more available space for pellets to evolve must have played an important role in this case too. At the same time the increasing initial amount of carbon source in the cultivation medium resulted in smaller morphological objects including clump forms and filaments that was previously

reported in literature for filamentous fungi (Nielsen et al., 1995; Papagianni, 2004). So it explains why the pellets in the run without glucose fell apart form the other runs with regard to their size and were the largest.

5. CONCLUSIONS

On the basis of the data presented in the work the following conclusions can be drawn.

1. *Streptomyces rimosus* is an actinomycete of rich secondary metabolism of potentially useful chemical substances.
2. Initial organic nitrogen (yeast extract) concentration much stronger affects the growth, morphological development and secondary metabolism of *S. rimosus* than initial carbon source (glucose) concentration.
3. The production of several metabolites depends on organic nitrogen concentration differently. Oxytetracycline and 2-acetyl-2-decarboxamidooxytetracycline are not produced at high organic nitrogen concentration while lorneic acid J, enaminomycin A and spinoxazine A are formed only at high concentration of organic nitrogen.
4. The formation of practically all found secondary metabolites of *S. rimosus* runs in accordance with the rule: the more carbon source, the more metabolite is formed.
5. Lack or deficiency of carbon source (glucose) affects the changes of pH level leading to the alkalisation of the cultivation medium, while a high amount of organic nitrogen (yeast extract) exerts opposite effect decreasing pH to acidic levels. Furthermore, instead of pellets, dispersed pseudomycelial morphology dominates at low pH. They could be the factors influencing the formation of secondary metabolites.

ACKNOWLEDGEMENTS

REFERENCES

Armstrong D.J., Scarbrough E., Skoog F., Cole D.L., Leonard N.J., 1976. Cytokinins in *Corynebacterium fascians* cultures: isolation and identification of 6-(4-Hydroxy-3-methyl-cis-2-butenylamino)-2-methylthiopurine. *Plant Physiol.*, 58, 749–752. DOI: 10.1104/pp.58.6.749.

Bizukojc M., Ledakowicz S., 2007. Simultaneous biosynthesis of (+)-geodin by a lovastatin-producing fungus *Aspergillus terreus*. *J. Biotechnol.*, 132, 453–460. DOI: 10.1016/j.jbiotec.2007.07.493.

Bizukojc M., Ledakowicz S., 2010. The morphological and physiological evolution of *Aspergillus terreus* mycelium in the submerged culture and its relation to the formation of secondary metabolites. *World J. Microbiol. Biotechnol.*, 26, 41–54. DOI: 10.1007/s11274-009-0140-1.

Bizukojc M., Pawlak M., Boruta T., Gonciarz J., 2012. Effect of pH on biosynthesis of lovastatin and other secondary metabolites by *Aspergillus terreus* ATCC 20542. *J. Biotechnol.*, 162, 253–261. DOI: 10.1016/j.jbiotec.2012.09.007.

Bode H.B., Bethe B., Höfs R., Zeeck A., 2002. Big effects from small changes: possible ways to explore nature's chemical diversity. *ChemBioChem,* 3, 619–627. DOI: 10.1002/1439-7633(20020703)3:7<619::AID-CBIC619>3.0.CO;2-9.

Boruta T., Ścigaczewska A., 2021. Enhanced oxytetracycline production by *Streptomyces rimosus* in submerged co-cultures with *Streptomyces noursei*. *Molecules*, 26, 6036. DOI: 10.3390/molecules26196036.

Boruta T., Ścigaczewska A., Bizukojć M., 2021. "Microbial wars" in a stirred tank bioreactor: investigating the co-cultures of *Streptomyces rimosus* and *Aspergillus terreus*, filamentous microorganisms equipped with a rich arsenal of secondary metabolites. *Front. Bioeng. Biotechnol.*, 9, 713639. DOI: 10.3389/fbioe.2021.713639.

Casas López J.L., Sánchez Pérez J.A., Fernández Sevilla J.M., Acién Fernández F.G., Molina Grima E., Chisti Y., 2003. Production of lovastatin by *Aspergillus terreus*: effects of the C:N ratio and the principal nutrients on growth and metabolite production. *Enzyme Microb. Technol.*, 33, 270–277. DOI: 10.1016/S0141-0229(03)00130-3.

Darken M.A., Berenson H., Shirk R.J., Sjolander N.O., 1960. Production of tetracycline by *Streptomyces aureofaciens* in synthetic media. *Appl. Microbiol.*, 8, 46–51. DOI: 10.1128/am.8.1.46-51.1960.

Del Carratore F., Hanko E.K.R., Breitling R., Takano E., 2022. Biotechnological application of *Streptomyces* for the production of clinical drugs and other bioactive molecules. *Curr. Opin. Biotechnol.*, 77, 102762. DOI: 10.1016/j.copbio.2022.102762.

Dinius A., Schrinner K., Schrader M., Kozanecka Z.J., Brauns H., Klose L., Weiß H., Kwade A., Krull R., 2023. Morphology engineering for novel antibiotics: effect of glass microparticles and soy lecithin on rebeccamycin production and cellular morphology of filamentous actinomycete *Lentzea aerocolonigenes*. *Front. Bioeng. Biotechnol.*, 11, 1171055. DOI: 10.3389/fbioe.2023.1171055.

Fu P., La S., MacMillan J.B., 2016. 1,3-Oxazin-6-one derivatives and bohemamine-type pyrrolizidine alkaloids from a marine-derived *Streptomyces spinoverrucosus*. *J. Nat. Prod.*, 79, 455–462. DOI: 10.1021/acs.jnatprod.5b00604.

Hochstein F. A., Schach von Wittenau M., Tanner Jr. F.W., Murai K., 1960. 2-Acetyl-2-decarboxamidoöxytetracycline. *J. Am. Chem. Soc.*, 82, 5934–5937. DOI: 10.1021/ja01507a034.

Itoh Y., Haneishi T., Arai M., Hata T., Aiba K., Tamura C., 1978. New antibiotics, enaminomycins A, B and C. III. The structures of enaminomycins A, B and C. *J. Antibiot.*, 31, 838–846. DOI: 10.7164/antibiotics.31.838.

Jiang Y., Zhang J., Huang X., Ma Z., Zhang Y., Bechthold A., Yu X., 2022. Improvement of rimocidin production in *Streptomyces rimosus* M527 by reporter-guided mutation selection. *J. Ind. Microbiol. Biotechnol.*, 49, kuac030. DOI: 10.1093/jimb/kuac030.

Jonsbu E., McIntyre M., Nielsen J., 2002. The influence of carbon sources and morphology on nystatin production by *Streptomyces noursei*. *J. Biotechnol.,* 95, 133–144. DOI: 10.1016/ S0168-1656(02)00003-2.

Jørgensen H., Nielsen J., Villadsen J., Møllgaard, H., 1995. Analysis of penicillin V biosynthesis during fed-batch cultivations with a high-yielding strain of *Penicillium chrysogenum*. *Appl. Microbiol. Biotechnol.*, 43, 123–130. DOI: 10.1007/BF00 170633.

Kodani S., Bicz J., Song L., Deeth R.J., Ohnishi-Kameyama M., Yoshida M., Ochi K., Challis G.L., 2013. Structure and biosynthesis of scabichelin, a novel tris-hydroxamate siderophore produced by the plant pathogen *Streptomyces scabies* 87.22. *Org. Biomol. Chem.,* 11, 4686–4694. DOI: 10.1039/c3ob40536b.

Kowalska A., Boruta T., Bizukojć M., 2018. Morphological evolution of various fungal species in the presence and absence of aluminum oxide microparticles: comparative and quantitative insights into microparticle-enhanced cultivation (MPEC). *Microbiol. Open*, 7, e00603. DOI: 10.1002/mbo3.603.

Li H., Hu Y., Zhang Y., Ma Z., Bechthold A., Yu X., 2023. Identification of RimR2 as a positive pathway-specific regulator of rimocidin biosynthesis in *Streptomyces rimosus* M527. *Microb. Cell Fact.*, 22, 32. DOI: 10.1186/s12934-023-02039-9.

Li Y., Lee S.R., Han E.J., Seyedsayamdost M.R., 2022. Momomycin, an antiproliferative cryptic metabolite from the oxytetracycline producer *Streptomyces rimosus. Angew. Chem.*, 134, e202208573. DOI: 10.1002/ange.202208573.

Lopez J.A.V., Nogawa T., Yoshida K., Futamura Y., Osada H., 2022. 2-Methylthio-N^7-methyl-cis-zeatin, a new antimalarial natural product isolated from a *Streptomyces* culture. *Biosci., Biotechnol., Biochem.*, 86, 31–36. DOI: 10.1093/bbb/zbab192.

Manwaring D.G., Rickards R.W., Gaudiano G., Nicolella V., 1969. The biosynthesis of the macrolide antibiotic lucensomycin. *J. Antibiot.*, 22, 545–550. DOI: 10.7164/antibiotics. 22.545.

McClure R.A., Goering A.W., Ju K.-S., Baccile J.A., Schroeder F.C., Metcalf W.W., Thomson R.J., Kelleher N.L., 2016. Elucidating the rimosamide-detoxin natural product families and their biosynthesis using metabolite/gene cluster correlations. *ACS Chem. Biol.*, 11, 12, 3452–3460. DOI: 10.1021/acschembio.6b00779.

Metz B., Kossen N.W.F., 1977. The growth of molds in the form of pellets – a literature review. *Biotechnol. Bioeng.*, 19, 781–799. DOI: 10.1002/bit.260190602.

Nielsen J., Johansen C.L., Jacobsen M., Krabben P., Villadsen J. 1995. Pellet formation and fragmentation in submerged cultures of *Penicillium chrysogenum* and its relation to penicillin production. *Biotechnol. Progr.*, 11, 93–98. DOI: 10.1021/bp00031a013.

Nonaka K., Tsukiyama T., Okamoio Y. Sato K., Kumasaka C., Yamamoto T., Maruyama F., Yoshikawa H., 2000. New milbemycins from *Streptomyces hygroscopicus* subsp. *aureolacromosus*: fermentation isolation and structure elucidation. *J. Antiobiot.*, 53, 694–704. DOI: 10.7164/antibiotics.53.694.

Ogaki M., Sonomoto K., Nakajima H., Tanaka A., 1986. Continuous production of oxytetracycline by immobilized growing *Streptomyces rimosus* cells. *Appl. Microbiol. Biotechnol.*, 24, 6–11. DOI: 10.1007/BF00266277.

Papagianni M., 2004. Fungal morphology and metabolite production in submerged mycelial processes. *Biotechnol. Adv.,* 22, 189–259. DOI: 10.1016/j.biotechadv.2003.09.005.

Pethick F.E., MacFadyen A.C., Tang Z., Sangal V., Liu T.T., Chu J, Kosec G., Petkovic H., Guo M., Kirby R., Hoskisson P.A., Herron P.R., Hunter I.S., 2013. Draft genome sequence of the oxytetracycline-producing bacterium *Streptomyces rimosus* ATCC 10970. *Genome Announc.*, 1, e00063-13. DOI: 10.1128/genomea.00063-13.

Petković H., Lukežic T., Šuškovic J., 2017. Biosynthesis of oxytetracycline by *Streptomyces rimosus*: past, present and future directions in the development of tetracycline antibiotics. *Food Technol. Biotechnol.*, 55, 3–13. DOI: 10.17113/ftb.55.01.17.4617.

Ramasamy S., Balakrishna H.S., Selvaraj U., Uppuluri K.B., 2014. Production and statistical optimization of oxytetracycline from *Streptomyces rimosus* NCIM 2213 using a new cellulosic substrate, *Prosopis juliflora. BioRes.*, 9, 7209–7221. DOI: 10.15376/biores.9.4.7209-7221.

Ścigaczewska A., Boruta T., Bizukojć M., 2021. Quantitative morphological analysis of filamentous microorganisms in cocultures and monocultures: *Aspergillus terreus* and *Streptomyces rimosus* warfare in bioreactors. *Biomolecules*, 11, 1740. DOI: 10.3390/biom11111740.

Seca A.M.L., Pinto D.C.G.A., 2019. Biological potential and medical use of secondary metabolites. *Medicines*, 6, 66. DOI: 10.3390/medicines6020066.

Seco E.M., Pérez-Zuñiga F.J., Rolón M.S., Malpartida F., 2004. Starter unit choice determines the production of two tetraene macrolides, rimocidin and CE-108, in *Streptomyces distaticus* var. 108. *Chem. Biol.*, 11, 357–366. DOI: 10.1016/j.chembiol.2004.02.017.

Shang N.-N., Zhang Z., Huang J.-P., Wang L., Luo J., Yang J., Peng T., Yan Y., Ma Y.-T. Huang S.-X., 2018. Glycosylated piericidins from an endophytic *Streptomyces* with cytotoxicity and antimicrobial activity. *J. Antibiot.*, 71, 672–676. DOI: 10.1038/s41429-018-0051-1.

Singh N., Rai V. Tripathi C.K.M., 2012. Production and optimization of oxytetracycline by a new isolate *Streptomyces rimosus* using response surface methodology. *Med. Chem. Res.*, 21, 3140–3145. DOI: 10.1007/s00044-011-9845-4.

Stephens C.R., Conover L.H., Hochstein F.A., Regna P.P., Pilgrim F.J., Brunings K.J., Woodward R.B., 1952. Terramycin. VIII. Structure of aureomycin and terramycin. *J. Am. Chem. Soc.*, 74, 4976–4977. DOI: 10.1021/ja01139a533.

Tesche S., Rösemeier-Scheumann R., Lohr J., Hanke R., Büchs J., Krull R., 2019. Salt-enhanced cultivation as a morphology engineering tool for filamentous actinomycetes: Increased production of labyrinthopeptin A1 in *Actinomadura namibiensis. Eng. Life Sci.,* 19, 781–794. DOI: 10.1002/elsc. 201900036.

van Santen J.A., Poynton E.F., Iskakova D., McMann E., Alsup T.A., Clark T.N., Fergusson C.H., Fewer D.P., Hughes A.H., McCadden C.A., Parra J., Soldatou S., Rudolf J.D., Janssen E.M.-L., Duncan K.R., Linington R.G., 2022. The Natural Products Atlas 2.0: a database of microbially-derived natural products. *Nucleic Acids Res.*, 50, D1317–D1323. DOI: 10.1093/nar/gkab941.

Vecht-Lifshitz S.E., Sasson Y., Braun S., 1992. Nikkomycin production in pellets of *Streptomyces tendae. J. Appl. Bacteriol.*, 72, 195–200. DOI: 10.1111/j.1365-2672.1992.tb01823.x.

Wu C., van der Heul H.U., Melnik A.V., Lübben J., Dorrestein P.C, Minnaard A.J., Choi Y.H. van Wezel G.P., 2019. Lugdunomycin, an angucycline-derived molecule with unprecedented chemical architecture. *Angew. Chem.,* 58, 2809–2814. DOI: 10.1002/anie.201814581.

Wucherpfennig T., Hestler T., Krull R., 2011. Morphology engineering – osmolality and its effect on *Aspergillus niger* morphology and productivity. *Microb. Cell Fact.,* 10, 58. DOI: 10.1186/1475-2859-10-58.

Yang R., Yang J., Wang L., Huang J.-P., Xiong Z., Luo J., Yu M., Yan Y., Huang S.-X., 2017. Lorneic acid analogues from an endophytic actinomycete *J. Nat. Prod.,* 80, 2615–2619. DOI: 10.1021/acs.jnatprod.7b00056.

Yin P., Wang Y.-H., Zhang S.-L., Chu J., Zhuang Y.-P., Chen N., Li X.-F., Wu Y.-B., 2008. Effect of mycelial morphology on bioreactor performance and avermectin production of *Streptomyces avermitilis* in submerged cultivations. *J. Chin. Inst. Chem.* Eng., 39, 609–615. DOI: 10.1016/j.jcice.2008.04.008.

Yin S., Wang X., Shi M., Yuan F., Wang H., Jia X., Yuan F., Sun J., Liu T., Yang K., Zhang Y., Fan K., Li Z., 2017. Improvement of oxytetracycline production mediated via cooperation of resistance genes in *Streptomyces rimosus. Sci. China Life Sci.,* 60, 992–999. DOI: 10.1007/s11427-017-9121-4.

Yu L., Cao N., Wang L., Xiao C., Guo M., Chu J., Zhuang Y., Zhang S., 2012. Oxytetracycline biosynthesis improvement in *Streptomyces rimosus* following duplication of minimal PKS genes. *Enzyme Microb. Technol.,* 50, 318–324. DOI: 10.1016/j.enzmictec.2012.03.001.

Zhao Y., Song Z., Ma Z., Bechthold A., Yu X., 2019. Sequential improvement of rimocidin production in *Streptomyces rimosus* M527 by introduction of cumulative drug-resistance mutations. *J. Ind. Microbiol. Biotechnol.,* 46, 697–708. DOI: 10.1007/s10295-019-02146-w.

Zygmunt W.A., 1961. Oxytetracycline formation by *Streptomyces rimosus* in chemically defined media. *Appl. Microbiol.,* 9, 502–507. DOI: 10.1128/am.9.6.502-507.1961.